Operando SXRD : a new view on catalysis

Ackermann, M.D.

III: Interaction between Pt(111), O_2 and CO at elevated pressure and temperature

In this chapter we present a series of SXRD experiments performed at high pressure and temperature on the Pt(111) single crystal surface. We have studied the interaction of CO and O_2 with this surface, as they form a classic model system for studying the catalytic oxidation of CO. We have studied the interaction of each single gas with the surface in the full range from UHV to atmospheric pressure. A very important result is the in-situ measurement of the oxidation of the Pt(111) surface, under formation of only several monoatomic layers of α-PtO_2. Secondly we have exposed the surface to mixtures of both gasses at elevated temperatures. We have measured the structure of the surface and its reactivity in the catalytic oxidation of CO simultaneously under semi realistic reaction conditions. The main result of this experiment is that we unambiguously show that the α-PtO_2 layer exhibits a much higher reactivity in CO oxidation than the bulk terminated Pt(111) surface.

3.1: Introduction

One of the main reasons for using the Pt(111) surface as a model surface is that it has a closed packed, hexagonal surface, which exhibits no surface reconstruction in clean UHV conditions. It has a simple 1x1 unit cell (figure (1)), and is relatively easy to clean under UHV conditions. Because of this, it forms a beautiful model system for the interaction between molecules and metal surfaces and the interaction between Pt(111), O_2 and CO has been studied widely in the past (e.g. [60,65,66] and the references therein). It is especially often used as a model system for heterogeneous catalysis, and the CO oxidation reaction on Pt is sometimes referred to a the 'fruit fly' of catalysis.

Early experiments under UHV conditions exposing the Pt(111) surface to both CO and O_2 have yielded a vast amount of data on the interaction between the Pt(111) surface and the reactant gas molecules for CO oxidation. But recent data from *in-situ* high pressure STM experiments have given a new impulse to the research on this catalytic system. Bobaru and coworkers have found that, in contrary to the common knowledge from the literature, the surface of a Pt(111) crystal forms an ultra-thin oxide layer under certain reaction conditions, which is catalytically much more active than the bare metallic surface [13,67]. Until now, oxide formation was believed to poison the catalyst (i.e. reduce the reaction rate) [82]. The Langmuir-Hinshelwood process that ran on the metallic surface was commonly seen as the active phase of the catalyst [60]. In this chapter we show with new High Pressure *SXRD* experiments, that indeed a Pt-oxide layer forms on the surface of Pt(111) under elevated pressure and temperature conditions. We confirm the findings of Bobaru *et al*. that this layer is a better catalyst for CO oxidation, exhibiting a much higher reaction rate for CO oxidation than the metallic surface. Secondly we find, in accordance to the work of Bobaru *et al*. that the reaction mechanism on this oxide surface is very different from the Langmuir-Hinshelwood mechanism found for the metallic surface.

3.2: Experimental

The experiments were performed at the ID03 beamline of the European Synchrotron Radiation Facility (ESRF) in the combined UHV - high pressure

SXRD chamber which is described in appendix A [48]. Inside the vacuum chamber, the sample was mounted on a BN heating plate and could be heated up to approximately 1300 K. Connected to the chamber was a gas manifold with four high-purity gasses (N47 grade for CO, N55 for all other). The chamber is also equipped with a quadrupole mass spectrometer (QMS) for online gas analysis. The setup was mounted on the z-axis diffractometer described in appendix B, with the crystal surface in a horizontal plane. A parallel beam of monochromatic, 17 keV X-ray photons was impinging on the surface at an angle of 1° (~ $2x10^{11}$ photons/s). The fluorescence radiation in the scattered beam was filtered with a crystal analyzer.

We describe the Pt crystal lattice with two unit vectors $\mathbf{A_1}$ and $\mathbf{A_2}$ which lie in the surface plane and which point respectively in the $[1\,\bar{1}0]$ and [-101] direction. A third vector $\mathbf{A_3}$ is perpendicular to the surface, and point in the [111] direction, i.e. the surface normal. $|\mathbf{A_1}| = |\mathbf{A_2}| = a_0 = 2.774$ Å. This is the Pt nearest-neighbor distance, and thus $\mathbf{A_1}$ and $\mathbf{A_2}$ span the surface unit cell of Pt(111). $|\mathbf{A_3}| = \sqrt{6}a_0 = 6.795$ Å. One can transform these vectors to reciprocal space by using equations 1a and b from chapter 3. The resulting reciprocal

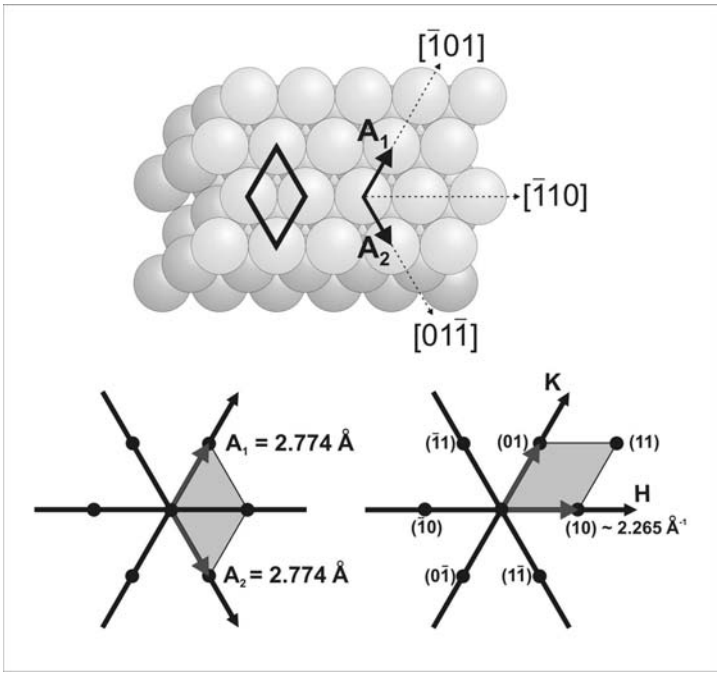

Figure 1: *Ball model and unit cell of Pt(111) spanned by $\mathbf{A_1}$ and $\mathbf{A_2}$ (top). Schematic unit cell in real space (left), and corresponding reciprocal space unit cell (right).*

space unit vectors are called **H** and **K** for the unit vectors that lye in the surface plane, and **L** for the vector along the surface normal. A ball model of the surface, together with a schematic drawing of both the real space and reciprocal space unit cell are shown in figure 1.

Well-ordered, clean Pt(111) surfaces were obtained after several ion bombardment (1 keV Ar^+) and annealing cycles. During the annealing cycles the surface was first heated to approximately 1050 K in a background pressure of 10^{-6} mbar of O_2 for 15 minutes to remove any carbon contamination. Subsequently the surface was flashed in vacuum to remove any adsorbed oxygen or oxide formed on the surface. After cooling, the cleanliness of the surface was checked Auger Electron Spectroscopy[i]. The crystalline quality of the surface was checked with *SXRD*. The full width at half maximum (*FWHM*) of a rocking scan around the surface normal at (*h k l*) = (1 0 0.5) was typically 0.07°, which corresponds to ordered domain (i.e. terraces) of linear dimensions of approximately 5000 Å.

3.3: Exposure to O_2

3.3.1: Low pressures of O_2

The clean Pt(111) surface was then exposed to O_2. The surface was first heated in vacuum to 425 K, and exposed to a pressure of 10^{-6} mbar of O_2. During this exposure, we measured no changes in the Crystal Truncation Rods (CTRs) of the Pt(111) surface with respect to the clean surface under vacuum conditions.

3.3.2: High pressure of O_2:

Keeping the surface at 425 K, we increased the pressure by factors of 10 starting form 10^{-6} mbar. Up to 10^{-1} mbar of O_2, no changes were observed in the diffraction signals, with respect to the clean surface in UHV conditions. When exposed to a pressure of 1.0 mbar of O_2 at 425 K, several changes are seen in the X-ray diffraction from the surface. New diffraction peaks appear along all

[i] *The Auger Electron spectroscopy was performed in a different UHV system, following the exact same sputtering and annealing procedure.*

main reciprocal space axes at ± 0.89 · **H** and ± 0.89 · **K** (figure 2), exhibiting a 60° degree symmetry (figure 3, top right, hollow points, grey diamond).

The in-plane unit cell formed by these new peaks in reciprocal space corresponds to a hexagonal unit cell in real space (figure 3, ball model). The length of the vectors spanning this unit cell in real space is $(0.89)^{-1} \cdot a_0 = 3.1$ Å. Such a unit cell corresponds very accurately to an α-PtO_2 unit cell, which has a hexagonal unit cell, with vectors of 3.113 Å [7]. Not taking the scattering of the oxygen atoms into account, this α-PtO_2 unit cell indeed exhibits a 60° degree symmetry. The surface was subsequently exposed to more elevated pressures of O_2 (10 mbar, 100 mbar, 1000 mbar) at the same temperature. At every increase of the pressure the diffraction from oxide layer grows slightly in intensity, going from sub-monolayer coverage at 1 mbar, to a couple of monolayers at 1000. The thickness and growth rate of the oxide layer also depends strongly on the temperature, but no systematic investigation of the growth or thickness as a function of temperature has been performed.

3.3.2.1: Orientation and commensurability

A data set of 5 rocking scans around the surface normal has been gathered. When ignoring the contribution of the oxygen in the α-PtO_2 unit cell on the scattering of the X-rays, only 2 of these peaks are non-equivalent. Due to the symmetry of the unit cell, the intensity and width of these peaks only varies due to the length of the diffraction vector $\boldsymbol{q}$, and this variation hence yields no information on the internal structure of the unit cell. From the width of rocking scans around the surface normal we can determine the average in-plane domain size within the α-PtO_2 layer. The typical theta scan of the oxide layer, shown in figure 2 of the first order diffraction peaks at (0.89 -0.89 0.5), shows a full width at half maximum (*FWHM*) of 6.5°. This corresponds to a linear domain size of 55Å. From this data set we conclude that the α-PtO_2 layer is oriented along the main crystallographic axes of the substrate. This can be expected from the fact that both the substrate and oxide layer share the same 120° degree symmetry (or 60° degree symmetry when only observing 1 single atomic layer of Pt(111)).

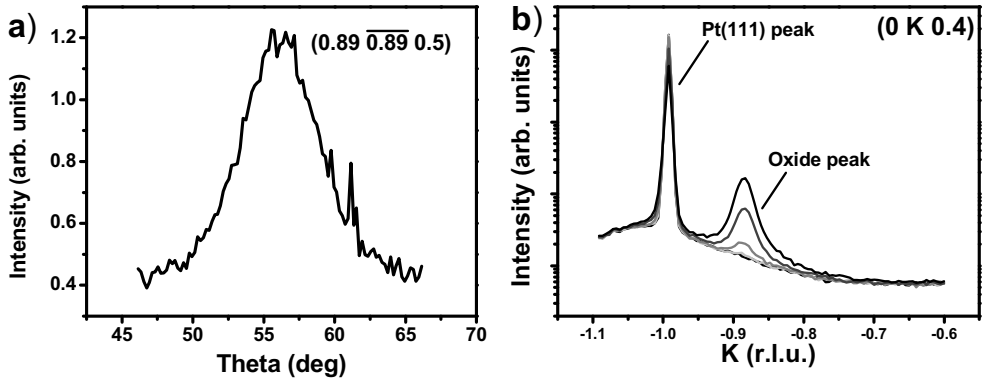

Figure 3: a) *Rocking scan around the surface normal of the oxide peak after exposure of the surface to 1.0 mbar of O_2 at 420 K.* ***b)*** *Superimposed series of scans taken at a 2 minute interval along the K direction during the growth of the oxide layer at 470K and 500 mbar of O_2, showing both the diffraction signal from the Pt(111) surface at K = -1 and from the growing oxide layer at K = -0.89.*

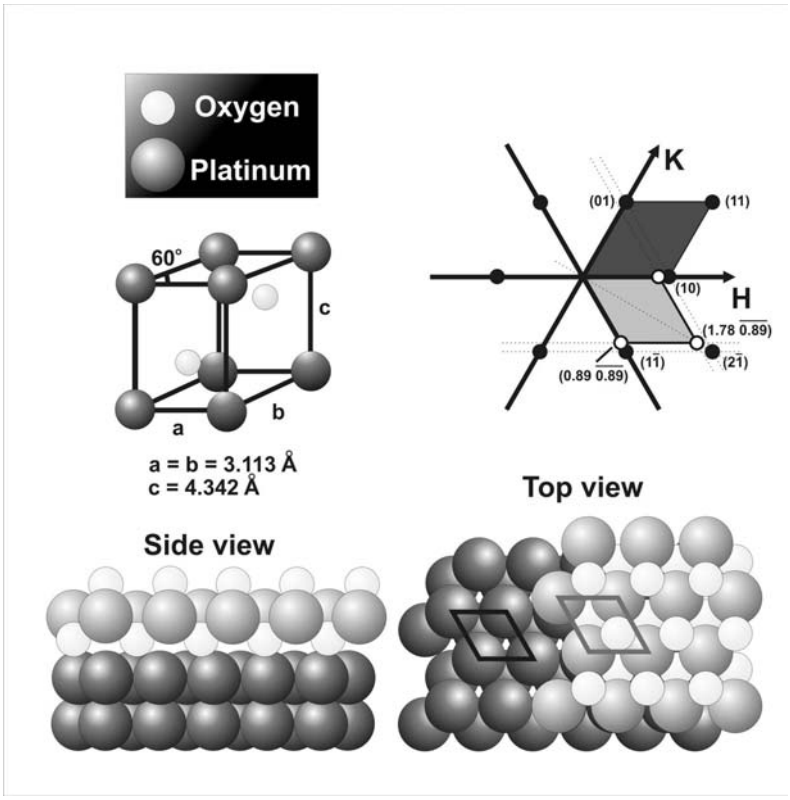

Figure 2: *Crystal structure of α-PtO_2 (top left). Measured in-plane reflections and reciprocal space unit cell of incommensurate α-PtO_2 layer (top right, grey unit cell, hollow white circles) and Pt(111) unit cell (dark grey, black circles). The α-PtO_2 is aligned along the crystallographic axes of Pt(111), but is incommensurate, showing peaks at* ***H*** *= 0.89,* ***K*** *= 0.89 and linear combinations thereof. Ball models of side and top view of a single O-Pt-O layer of α-PtO_2 on the Pt(111) surface. The top view also shows the real space in-plane unit cells of both oxide (grey) and metallic surface (black).*

Although well oriented, the oxide layer is incommensurate with respect to the substrate, as it shows no coincidence lattice with the Pt(111) in-plane lattice. From the ratio of the respective unit cell sizes, one could argue that an extended (8x8) or (9x9)-α-PtO_2 cell would coincide with respectively a (9x9) or (10x10) unit cell of the underlying Pt(111) and nicely describe the epitaxial relationship between both structures. Unfortunately, the average domain size within the oxide layer (see here above) is of the same order as such an "(8x8) on (9x9)" coincidence cell. So, although such a cell would fit nicely, it is not expected to have a real structural influence on the structure of the α-PtO_2 layer on this surface.

No further fitting has been done to the data to try to improve or further detail the in-plane structure of this oxide layer. One only possible addition would have been to fit the position of the oxygen atoms within the unit cell. Unfortunately, contribution of the oxygen atoms to the total diffracted intensity is relatively moderate, as the diffracted intensity scales with the square of the number of electrons around an atom. A small movement of the Pt atoms within the unit cell will have a similar effect on the diffracted intensity as completely removing the oxygen atoms. Because of this, our fitting procedure is not very sensitive to the position or presence of the oxygen atoms within the unit cell. In all calculations, the oxygen atoms have been put at their expected (bulk) position, and these positions have not been allowed to relax during the fitting procedures.

3.3.2.2: Thickness

In the case of the growth of such an oxide layer on a smooth, single crystal metal surface, several methods can be used to determine its thickness, and out-of-plane properties with *SXRD*. The most accurate and robust method is to measure the specular reflectivity of the surface. Put in HKL coordinates this is equivalent to measuring a (*0 0 l*)-scan. The growth of a layer of a finite thickness and with a different electronic density than the bulk of the substrate can very accurately be determined with this reflectivity measurement. Both the thickness and the electronic density of the layer can be determined from the features of the reflectivity curve [17,39,68].

A specific feature of the reflectivity is that it is only sensitive to the out-of-plane structure of the surface and totally insensitive to any in-plane structure due to the fact that the in-plane component of the diffraction vector $\boldsymbol{q}$ is 0. At

any point along the (*0 0 l*)-scan $\boldsymbol{q}$ always points exactly in the direction of the surface normal, hence probing the variation in electronic density in that direction only. This is shown in the schematic drawing of figure 4. The (only) two values to which a reflectivity curve is sensitive, and hence that can be determined from such a measurement are the layer positions of the newly grown layers, or as shown in figure 4 the position of the surface(oxide) layers $\mathbf{p_1}$ to $\mathbf{p_4}$ and the electronic density of these layers, depicted as $\mathbf{e_1}$ to $\mathbf{e_4}$. These two parameters per layer fully determine the diffracted intensity measured in a (*0 0 l*)-scan. To see the effect of these parameters we can simulated the reflectivity of a clean Pt(111) surface and an oxide-covered surface. The effect of varying the different parameters is shown in figures 5(a) and 5(b). For these simulations, a Pt(111) bulk and 4 Pt(111) "surface layers" have been chosen. By varying the occupancy number of these surface layers with respect to bulk Pt(111) from 0% ('empty') to 100% (bulk Pt(111)) oscillations appear as a function of the out-of-plane reciprocal space vector **L**. The depth of the oscillations along the (*0 0 l*) curve changes (figure 5 (a)) as a function of this occupancy number, nicely showing the 'bulk' reflectivity at both 0% and 100%, and the strongest oscillation at 50% occupancy. The exact position of the minima along the reflectivity curve is sensitive to the spacing between two oxide monolayers, the total thickness of the oxide layer and the distance between the oxide layers and the Pt(111) bulk. In figure 5 (b) a simulation is shown in which the interlayer distance within the oxide is varied. Obviously, several equivalent methods exist for defining and fitting these parameters. If we fix the electronic density of each new layer to that of α-PtO_2, and vary a so-called occupancy number, we can fit the thickness of the oxide layer in numbers of fully and partially filled monolayers of oxide. The position of each oxide layer can be varied individually, or we can assume an isotropic crystal, simplifying the position of the layers to two parameters: the distance of the first layer with respect to the Pt(111) surface, and a constant interlayer distance. The measured reflectivity data from the Pt(111) surface after exposure for to 500 mbar of pure oxygen at 400 K is shown in figure 5(c). As a reference the clean, smooth, bulk terminated Pt(111) surface in UHV conditions is also shown in figures 5 (c) and (d).

From the oscillations along the curve, it is clear that a layer of "non-bulk" material has grown on the surface. Fitting these oscillations with the method and model described here above results in the grey, continuous curve, which describes the data relatively well (solid grey curve).

This fit shows that this oxide layer is 6.7 Å thick, with an average electronic density of 2.9 $e^-/Å^3$. This corresponds to approximately 1.5 monolayers of oxide. Adding one extra layer in the fit procedure did not improve the fit significantly, and showed an occupancy for this last layer of below 5%. Figure 5(d) shows the reflectivity from the Pt(111) surface after exposure to 500 mbar of pure oxygen at 575 K. From the spacing between the minima of the oscillations we can immediately conclude that the oxide layer is thicker than the one causing the oscillations shown in figure 5(c). Fitting this intensity curve with the same method as described for figure 5(c) yields a very good fit to the data (continuous grey curve). In this case the best fit is achieved for an oxide slab composed of 11.6 Å, which corresponds to a slab of 2 to 3 α-PtO_2 oxide layers. Adding one extra monolayer of α-PtO_2 to the fit did not improve the fit significantly, and gave an occupancy number close to 0% for this outermost

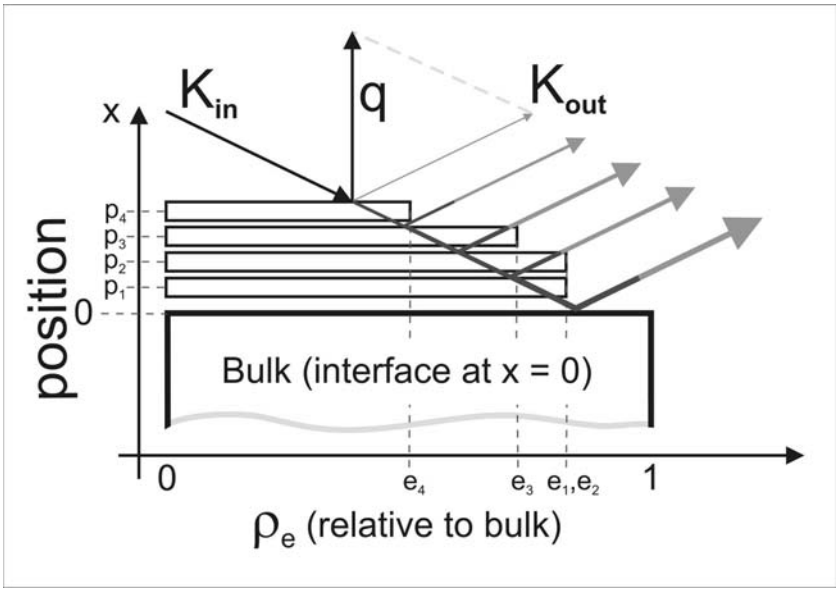

Figure 4: *Schematic model for specular diffraction from a bulk terminated surface plus several layer of 'oxide'. Only two parameters influence the diffracted intensity: The electronic density (ρ_e), and the position of the oxide layers. The electronic density influences the total diffracted intensity from one single layer. The position of each layer influences the (extra) path length of the diffracted signal (dark grey), and hence its phase. The bulk material has an electronic density of '1', a full layer of the oxide has a density of 'e_1'. Non-filled layer of the oxide have an effective electronic density of less than e_1. The combination of position and electronic density of each new layer fully determines the change in diffracted intensity with respect to a clean bulk-terminated surface.*

oxide layer. The average electronic density of this layer is 3.02 $e^-/Å^3$. We must note that the best fit shows a variation of approximately 20% of the electronic density between the different O-Pt-O tri-layers within the oxide slab. From the literature values for the unit cell of α-PtO_2 we can calculate that the theoretical bulk electronic density for α-PtO_2 should be 3.02 $e^-/Å^3$. This matches perfectly with the values found in both fits. Both fit show a very high roughness for this oxide slab. The fit yielded a value for 'beta' (approximated beta-roughness model) of 0.55.

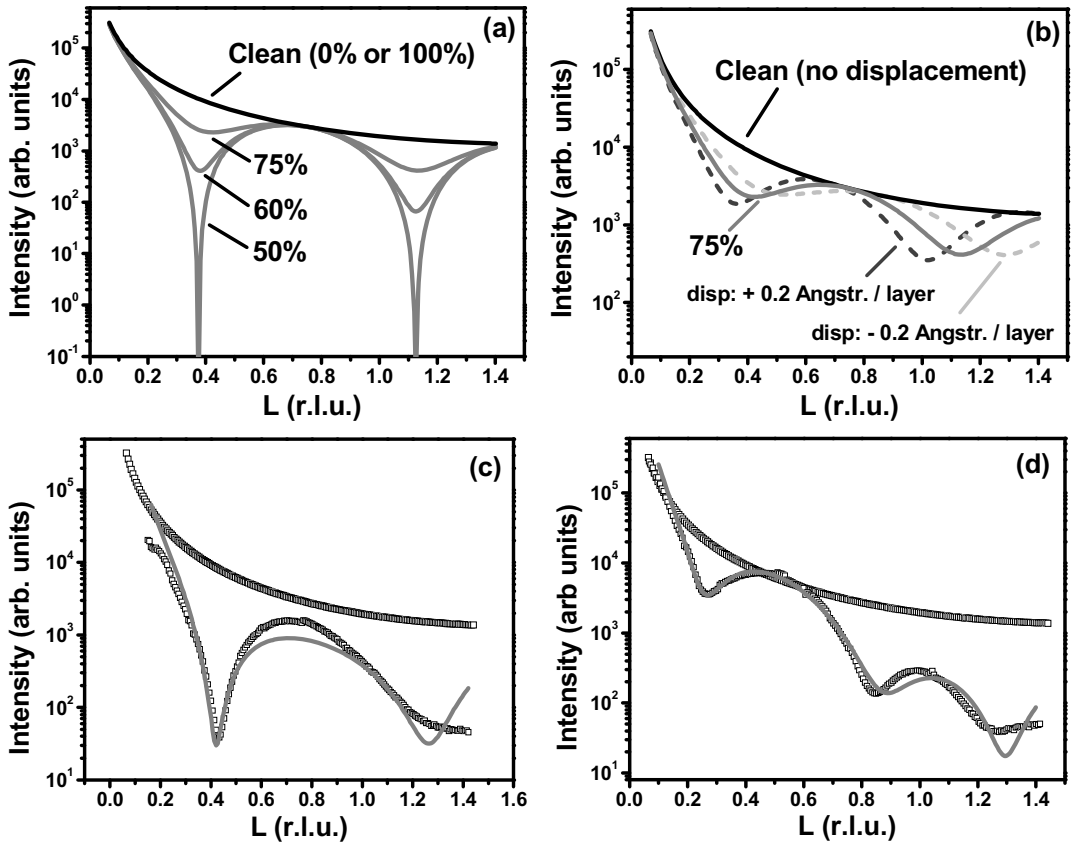

Figure 5: *Simulations and real measured specular reflection data.* ***a)*** *A simulation of 4 layers of 'oxide' on a Pt(111) bulk terminated crystal. By varying the electronic density from 100% to 0% of the bulk electronic density the 'depth' of the oscillations along the 00L curve vary.* ***b)*** *Changing the position of the 4 oxide layers by stretching or contracting the interlayer distance within the oxide slab varies the period of the oscillations along the 00L curve (example given for a simulated oxide layer with an electronic density of 75% of bulk Pt(111)).* ***c)*** *Diffracted intensity for a relatively thin oxide layer on Pt(111), grown at 500 mbar of O_2 and 400 K, together with the diffracted intensity of a clean, smooth, bulk terminated Pt(111) surface. The grey line is the best fit, representing 1.5 ML of α-PtO_2.* ***d)*** *Diffracted intensity for a relatively thick oxide layer on Pt(111), grown at 500 mbar of O_2 and 580 K, together with the diffracted intensity from a clean, bulk terminated Pt(111) surface. The grey line is the best fit, representing 2.7 ML of α-PtO_2.*

3.3.2.3: Growth oscillations

The method shown here above allows us to determine the thickness of the oxide layer at a given moment in time. It is very accurate as long as the thickness of the oxide layer does not vary (significantly) during a single (0 0 L)-scan, i.e. when the oxide layer thickness is constant as a function of time. When the oxide layer is still growing significantly as a function of time, we can monitor the growth of the layer by using the *SXRD* signal to measure so-called 'growth oscillations' [68]. These are oscillations of the diffracted intensity at a specific point in reciprocal space as a function of time, and not as a function of the diffraction vector $\boldsymbol{q}$. These oscillations are very comparable with RHEED oscillations.

Normally, these oscillations are used to monitor commensurate epitaxial growth, or even homo-epitaxial growth processes. When a commensurate overlayer grows on a substrate, one can find specific positions in reciprocal space where there is interference between the signal of the substrate *and* the growing layer. From the variation of this signal as a function of time, one can monitor the growth with sub-monolayer precision. Even though in this case the α-PtO_2 and the Pt(111) substrate are incommensurate with respect to each other, we can still see the effect of the oxide growth on the diffraction signal coming from the Pt(111) surface, and quantify the growth speed of the oxide layer with the variation in this signal.

The explanation for this is straightforward: At the "anti-phase" point of a CTR, exactly between two volume Bragg peaks, the diffracted X-Rays from each subsequent atomic layer are exactly out-of-phase with the diffracted X-Rays from the next one. Taking this destructive interference into account, and combining it with the absorption of the X-Rays at every layer of the crystal, we can calculate the total diffracted intensity at the "anti-phase" of a single crystal, with a 'perfect' surface. We find at this "anti-phase" an intensity which corresponds to the diffraction from exactly 0.5 ML (see this thesis, chapter 1.6.2) [39,68].

When growing a homo-epitaxial layer on this perfect single crystal surface, the diffraction from the atoms deposited in the new, growing layer is out-of-phase with the signal coming from the substrate. This means that the deposition of each new atom will make the intensity drop from its initial (maximum) value of 0.5 ML, until exactly 0.5 ML is deposited. At that point the intensity at the anti-phase will be 0. All atoms deposited beyond that point will make the intensity

increase again until a full layer is reached, and the intensity is back at the original value of 0.5 ML. A schematic representation of this homo-epitaxial growth is shown in figure 6(a).

During the growth, the structure factor F varies linearly with the amount of deposited material or coverage θ. θ is defined as the partial coverage of the new layer, where $\theta = 0$ means an empty layer and $\theta = 1$ is a fully filled layer. For simplicity, we have normalized $F(\theta)$ to run from 0 to 1 in all calculations and simulations. Excluding negative values for $F(\theta)$ we then get:

$$F(\theta) = 2 \cdot \left| 1/2 - \theta \right| \qquad (2a)$$

The intensity $I(\theta)$, which scales as F^2, will exhibit a parabolic behavior as a function of θ:

$$I(\theta) = (F(\theta))^2 = 4 \cdot \left(1/2 - \theta \right)^2 = 4 \cdot \left(\theta^2 - \theta + 1/4 \right) \qquad (2b)$$

In *SXRD* experiments these parabolic shaped oscillations of the intensity are a typical footprint for homo-epitaxial "layer-by-layer" growth [68]. Normally these intensity-oscillations are measured as a function of time, giving a straightforward method for calculating the coverage $\theta(t)$. Figure 7 shows the behavior of $F(t)$ (middle panel) and $I(t)$ (bottom panel) as a function of time for a constant deposition rate, and for the growth of one single ML. Of course this is in the highly hypothetical case of 'perfect' layer-by-layer growth where the new layer starts to grow only after the previous one has completely finished covering the substrate surface.

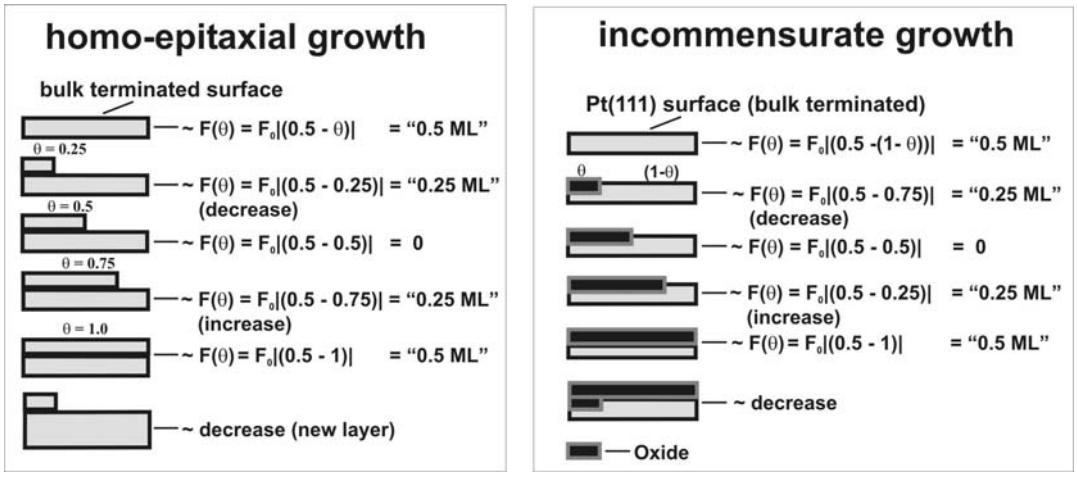

Figure 7: *left panel: Schematic drawing of perfect, layer-by-layer homo-epitaxial growth (Frank – van der Merwe growth). Next to the model the behavior of F(θ) as a function of the growth of that single layer is calculated. Right panel: Schematic drawing of the growth of an incommensurate layer on Pt(111). By taking atoms from the top layer of a bulk terminated crystal, and incorporating them in the incommensurate layer, material is 'removed' from this first layer. The coverage of the incommensurate θ layer is the complement to the amount of material remaining in the top layer (1-θ). The behavior of F(θ) as a function of the remaining material is calculated, and is exactly equal to the behavior of F(θ) during homo-epitaxial growth.*

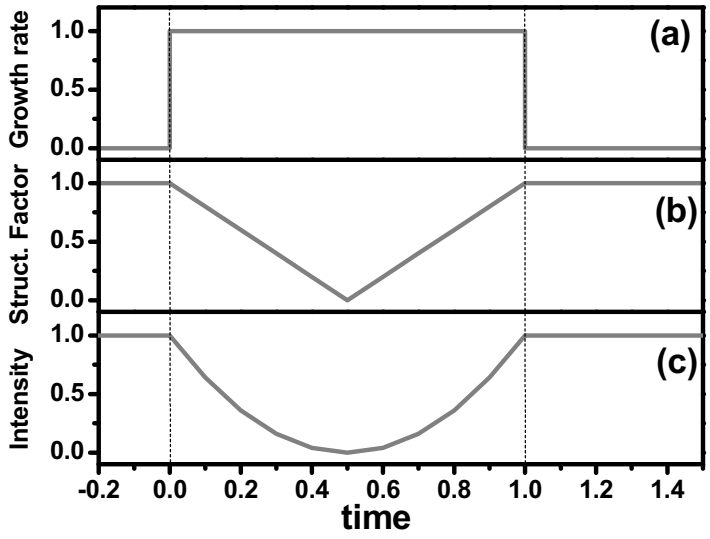

Figure 6: a) *Simulation of the growth of a single mono-atomic layer (growth rate in ML / time unit).* ***b)*** *Calculated behavior for the structure factor at the anti-phase of a CTR during perfect layer-by-layer growth of a single ML.* ***c)*** *Parabolic behavior of the intensity at the anti-phase point of a CTR, calculated from the structure factor shown in b.*

In our case, although we are not dealing with homo-epitaxial growth, but with the growth of an incommensurate layer, we can still apply this same model. A schematic drawing of this process is shown in figure 6 (right panel). In the incommensurate case, it is not the material deposited on the surface which is responsible for the change in diffraction intensity at the anti-phase, but the removal of Pt atoms from the Pt(111) surface to form the oxide layer. As the Pt atoms that constitute the oxide layer do not contribute any more to the intensity of the Pt(111) CTR's, we can now consider θ as the Pt *remaining* in the outermost Pt(111) layer, instead of the material being deposited. The only difference being that θ now runs from 1 to 0, but as we can see from equation 2a and 2b, this is fully equivalent to the homo-epitaxial deposition case.

A measurement of the intensity at the anti-phase of a Pt(111) CTR is shown in figure 8. The measurement of the CTR as a function of time clearly shows the change in intensity at the anti-phase (figure 8a and b), but does not allow us to fully monitor the shape of the growth oscillation as a function of time.

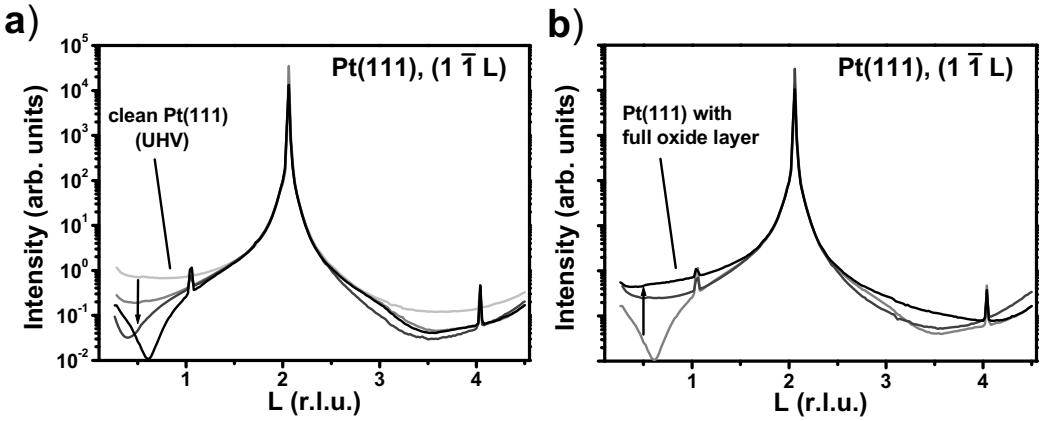

Figure 8: *Intensity oscillations due to the growth of an incommensurate oxide layer at 510 mbar of O_2 and 600 K.* ***a)*** *Scans along the* ***L*** *direction at different moments during the initial growth stage. The time runs from the light gray line (t = 0, reference scan) to black (minimum in intensity). The intensity at the anti-phase is decreasing as a function of time, hence the oxide layer is taking up from 0 to 0.5 ML from the Pt(111) surface.* ***b)*** *Scans along the* ***L*** *direction at different moments during the growth of the oxide layer. Again time runs from the light gray line to the black one. The growing intensity indicates that the oxide layer is taking up between 0.5 and 1 ML of the surface.*

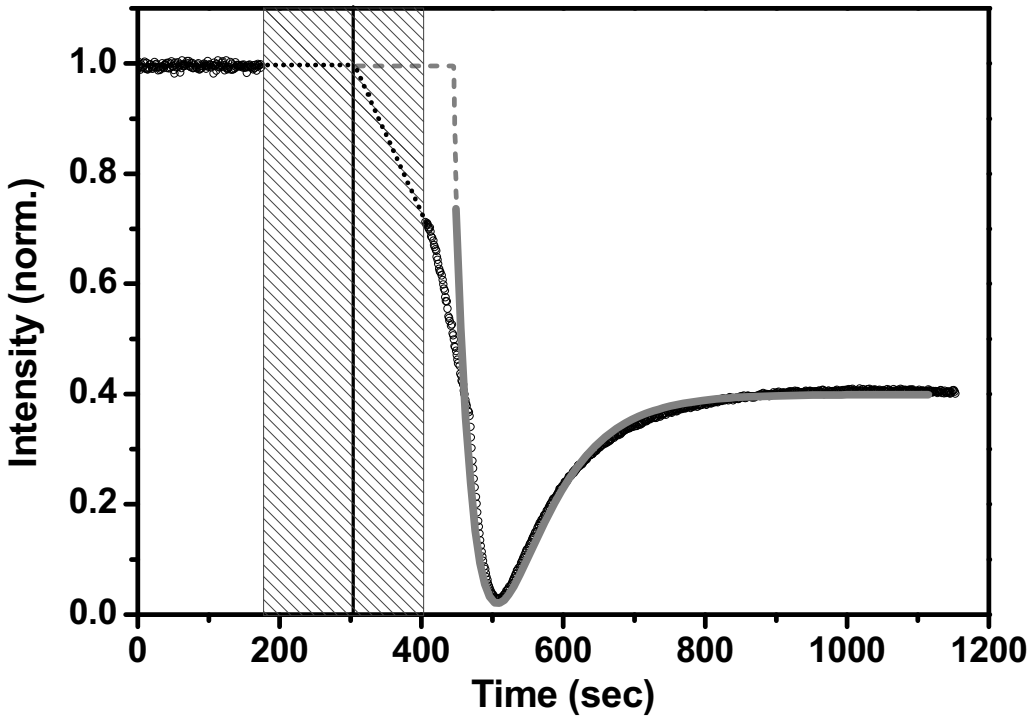

Figure 9 *The intensity oscillation not as scan along* ***L****, but as a function of time with the detector fixed at the anti-phase position (1 -1 0.5) (hollow circles) at 510 mbar of O_2 and 600 K. The surface is exposed to this pressure of O_2 from approximately t = 300 sec (black vertical line in the hatched area). The intensity signal before t = 200 is used to normalize the intensity of the clean surface to 1. No diffraction data have been measured between t = 200 and t = 400 sec (hatched area). The grey continuous line is a fit for a kinetically hindered growth, giving an exponentially decaying growth rate (see figure 9), with a final total coverage of 0.2 ML of Pt(111) (i.e. 0.8 ML of oxide). The kinks in the slope of the diffracted intensity around t = 400 and t = 460 are due to an increase in intensity of the X-Ray beam. A t = 400 the measurement started, and at t = 460 a filter was removed from the beam, increasing the intensity of the X-Rays by a factor of 3. At this O_2 pressure the growth rate is influenced by the presence of the X-Ray beam. For the fit only the points after t = 460 have been taken into account. Fitting the growth before t = 460 has no real interest as that part is very well described by a straight line, and hence represents the linear part of the exponential decay. The black dots in the hatched area are not measured intensities, but represent linear extrapolations of the measured intensities before, and after the exposure to the oxygen and serve as lines to guide the eye. The grey dashed line is an extrapolation to the starting point of the fit for the fastest growth rate under full X-Ray illumination.*

A second measurement has been performed, not measuring the full CTR, but only the intensity at the anti-phase as a function of time. This is shown in figure 10. It is clear from figure 10 that the intensity oscillation does not exhibit a perfect parabolic behavior. The deviation from this behavior can be explained due to 2 factors. The first one is the growth rate of the oxide layer: the oxide growth at this temperature and oxygen pressure is kinetically limited [47], due to the lack of bulk diffusion. Because of this, the growth rate of the oxide layer will not be constant is time, but show an exponential decay. The effect of the exponentially decreasing growth rate is shown in figure 10. The decreasing growth rate has a direct influence on $\theta(t)$ (figure 10b). Putting this behavior of θ as a function of time into equations 2a and 2b we can retrieve the values for $F(t)$ and $I(t)$ during the growth (figure 10c and d). The resulting shape of $I(t)$ (figure 10d) is already much more similar to the shape presented in figure 9. A second effect that has to be taken into account in the oxide growth case is that the growth does not need to stop at exactly integer values for θ, but will in most

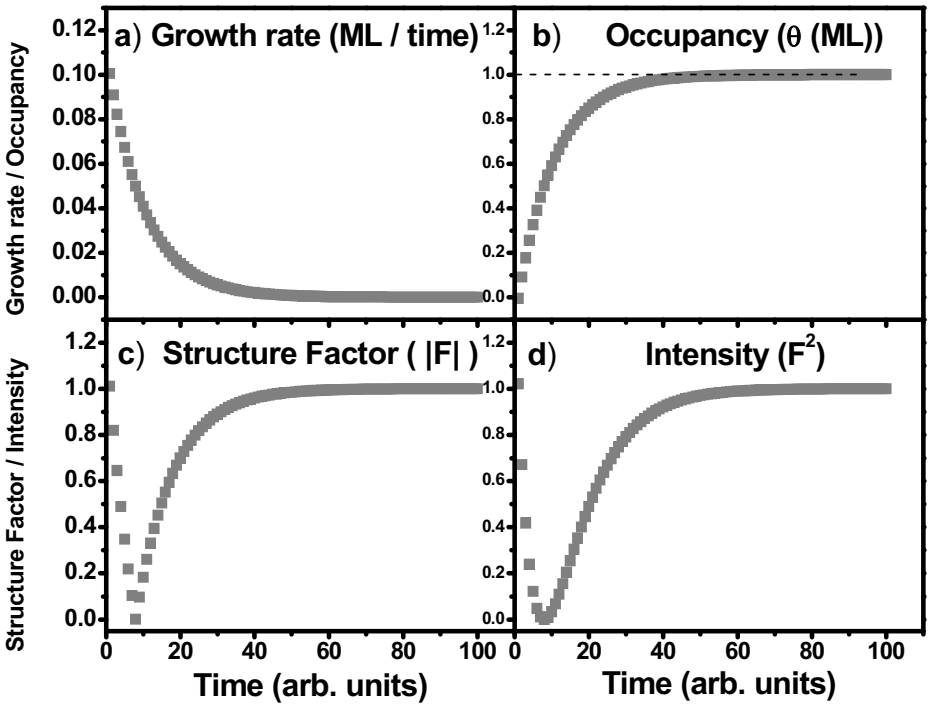

Figure 10: *Deviation from perfect layer-by-layer growth as shown in figure 7. For a kinetically hindered growth of 1 full ML, the growth rate decreases as a function of time* ***(a)****. The corresponding occupancy is shown in* ***(b)****. From* ***(b)*** *we calculate the structure factor |F| at the anti-phase* ***(c)****, and from the structure factor we get the intensity* ***(d)****. This is still for perfect layer-by-layer growth, with 0 roughness, and exactly 1 single ML.*

cases stop at a fractional coverage of the surface, and hence at a fractional value of θ. Putting these two effects in a simple calculation allows to fully characterize the growth oscillation of the oxide layer as shown in figure 9. The grey continuous line in figure 9 is a calculation for the intensity *I(t)* for an exponentially decaying growth rate as shown in figure 8, and a value for θ at t = 1200 of 0.2 ML, i.e. an 0.8 ML coverage for the oxide layer. We can see that this mechanism fits the data of figure 9 very well. This shows that we are indeed dealing with a kinetically limited growth rate.

NB: This method only gives information about the growth rate of any incomplete oxide layer, as we are insensitive for full layers of oxide (or actually fully 'empty' layers of Pt(111)). We can hence not conclude anything about the total thickness of the oxide film with this method.

3.3.2.4: Beam effect

Figure 9 shows a very good agreement between the fit and the experimentally measured growth curve, but only in the part of the curve from t = 460 seconds onwards. There is a clear inflection in the curve at t = 460. The growth rate *before* t = 460 is clearly slower than after that point. The sudden acceleration in the growth seen in this figure of the oxide layer is due to a beam effect. The inflection in the curve of figure 9 exactly coincides with the removal of 1 attenuator from the beam. This should have no effect on the measured intensities as *I* is corrected for the presence of the attenuators, so apparently it is the growth rate itself that is truly affect by the change in intensity of the X-Ray beam. This effect is not a local effect, as we have measured that the whole surface exhibits the same oxide layer thickness, and is hence attributed to a general effect of the presence of the X-Rays with the gas phase. As the gas phase is solely composed of O_2, we attribute the acceleration to the formation of a more oxidizing agent than O_2 in the gas phase by the X-Ray beam, which could be atomic oxygen, but most probably ozone (O_3).

The beam effect has been seen in all intermediate pressure experiments (10^{-1} - 10 mbar O_2). In all these experiments, it is very difficult to determine if any oxide growth would have taken place at all without the presence of the X-Ray beam. In more elevated pressure conditions (> 100 mbar) the beam effect is negligible with respect to the oxide growth with no (or minimal) presence of the X-Ray beam. No clear statement can hence be made about the exact pressure at which the oxide growth initiates.

3.4: Exposure of α-PtO_2 to CO

One of the main reasons to look at the oxidation of the Pt(111) surface under high oxygen pressure conditions is the role that this oxide layer plays in the reactivity of a Pt catalyst in the conversion of CO to CO_2. Several publications have already shown that an atomically thin oxide layer is, under specific high pressure and temperature conditions, a much better catalyst than the gas-covered metallic surface. This is the case for example for Pt(110) [10,62], Pd(100) [10,69], and Ru(0001) [6]. In many of the experiments however, it is relatively difficult to make a direct link between the oxide layer and the exhibited reactivity. In some cases, no real reactivity is measured, only the traces the reaction has left on the surface [2], or real reactivity is measured but it is very difficult to identify the (structure of the) oxide. Using the combination of the *SXRD* and a mixture of O_2 and CO in the high pressure chamber [48], monitored with a Quadrupole Mass Spectrometer (QMS) we can make a direct link between the reactivity exhibited by the surface, and the surface structure, under these high pressure (approximately 1 bar total pressure), and high temperature conditions (425 – 600 K). Several reactivity experiments have been performed under different pressure and temperature conditions. These reactivity experiments have all been performed in the following way: The Pt(111) crystal was prepared under UHV conditions until large and flat terraces were measured, and no other diffraction peaks than those from the Pt(111) surface could be detected. Subsequently the surface was exposed to 500 mbar of oxygen at 580 K (± 20 K). Under these conditions, an α-PtO_2 slab of several ML formed on the surface within approximately 15 minutes. Once the oxide growth rate had slowed down to below any detectible growth within the detection limit of the X-Rays[ii], we chose the temperature at which we would conduct the reactivity experiment, and let the oxide covered surface heat or cool to the chosen temperature. Once the temperature was stable, we exposed the surface to a series of CO pulses, depicted in figure 11a with the labels “a” to “f”. The gas phase in the reactor is then composed of 400 mbar of O_2 (figure 11a, light gray line), and a relatively small amount of CO (figure 11a, black line). At the start of the experiment no CO_2 is present in the reactor

[ii] *The X-Rays allow a detection of less than 5% of a monolayer of oxide. If no change in the detection signal is measured for approximately 5 to 10 minutes, we consider the growth rate to be 0. This combines to a detectable growth rate of less than* $5*10^{-3}$ *ML/min.*

(figure 11a, dark grey line), but as the CO reacts to CO_2, the reactor slowly fills up with this reaction product.

At “a” a CO pulse of 2 mbar is added to the reactor. It immediately starts reacting under formation of CO_2 (CO pressure drops, CO_2 rises), which shows that the catalyst is working properly. The first CO pulses are kept relatively low, typically in the range of 10 to 20 mbar (figure 11c “a” - “c”). Almost no variation in the diffracted intensity from both the oxide layer an the Pt substrate is detected. From this we conclude that the surface is fully covered by the oxide layer during these first pulses. The only possibility then for CO to react to CO_2 is by either finding oxygen atoms adsorbed on the oxide layer, or by reacting with the oxygen atoms of the oxide layer itself.

The only variation in diffracted intensity during these initial pulses is a gradual lowering of both the oxide and metal diffraction peaks, which points towards a gradual roughening of the surface [6,9,10,13,62,67,69]. From this roughening we conclude that CO must react with the oxygen atoms *within the oxide layer*, as a roughening of the surface cannot be explained by reaction with chemisorbed of physisorbed oxygen. This reaction path, where one species reacts with an atom from the substrate itself, and not with an adsorbed molecule or atom is called the “Mars-Van Krevelen” (MvK) mechanism [4]. This mechanism implies that the oxide layer is continuously reduced by the CO molecules at the rate of CO_2 production. To retain the full diffraction intensity from the oxide layer while the CO molecules continuously reduce it, the Pt atoms in the oxide layer must be “re-oxidized” by oxygen from the gas phase. To retain a full oxide layer (or several monolayers) this oxidation process must be faster than the reduction process.

For CO oxidation on late transition metals this mechanism has already been proposed in a number of publications [6,9,10,13,62,67,69]. In all the experiments described in these publications it has been shown that the roughening of the surface during catalytic CO oxidation is caused by the MvK reaction mechanism. A schematic illustration of the MvK mechanism and the subsequent roughening process is shown in figure 6 of chapter 3.

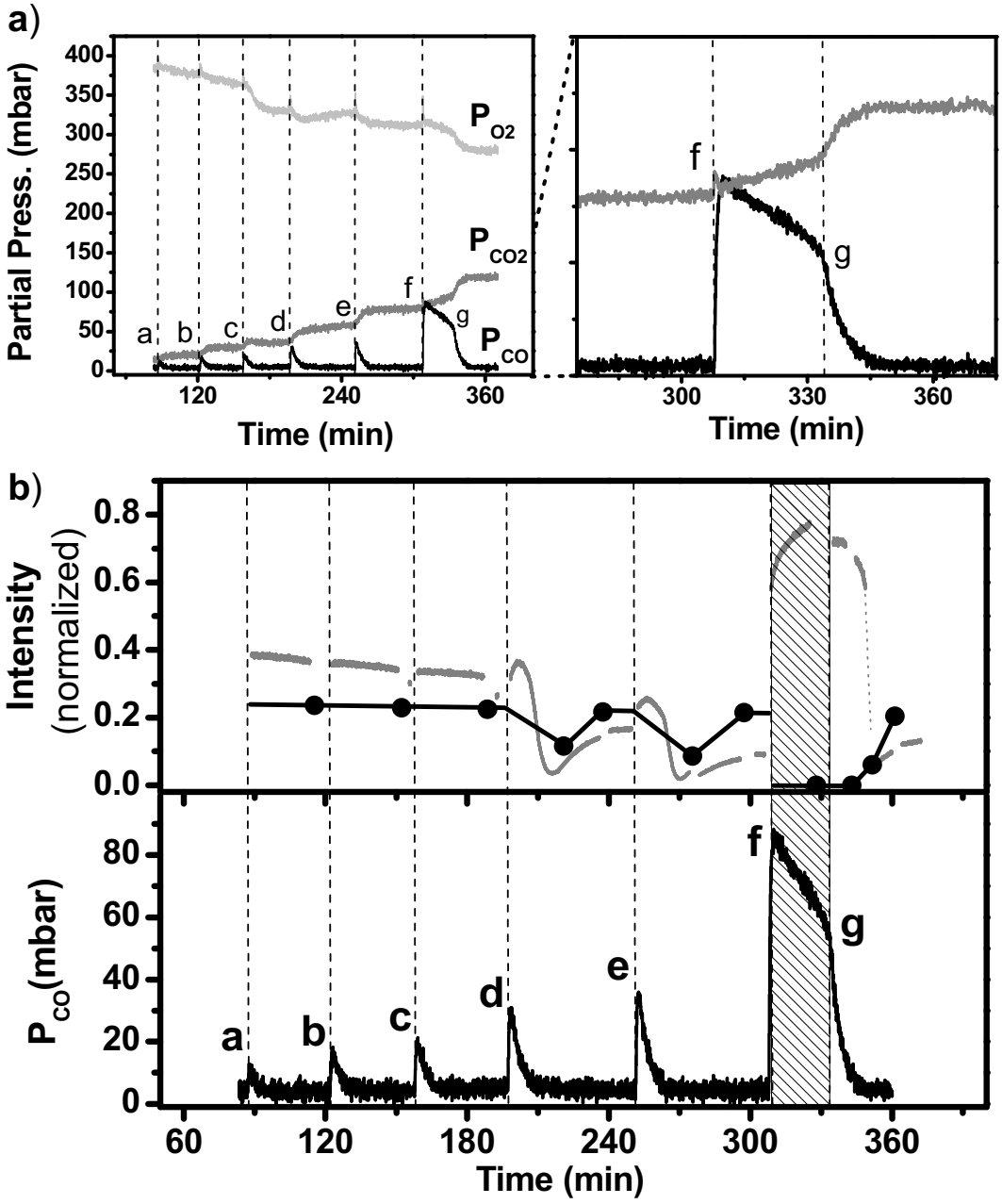
a)
Partial Press. (mbar)
400
350
300
250
200
150
100
50
0
P_{O2}
P_{CO2}
P_{CO}
a
b
c
d
e
f
g
120
240
360
Time (min)
f
g
300
330
360
Time (min)
b)
Intensity
(normalized)
0.8
0.6
0.4
0.2
0.0
P_{CO}(mbar)
80
60
40
20
0
a
b
c
d
e
f
g
60
120
180
240
300
360
Time (min)

Figure 11: a) *Pulse experiment starting in 400 mbar of O_2 (light grey line) with increasing doses (pulses) of CO (black line) at 600 K. After each pulse, the CO and O_2 pressure immediately start decreasing and the CO_2 pressure increases (grey line), showing that the catalyst is working properly. The decrease in CO pressure shows an exponential decreasing behavior in time for the pulses labeled "a" to "e", indicating that the reaction rate is linear with the CO pressure. At pulse "f" (see also zoomed panel) the reactivity changes drastically. It is much slower than expected for the linear reaction rate dependence, and it does no longer show an exponential decay in time. At "g" the reaction rate reverts to the higher rate, and exponential decay in time.* ***b)*** *Combining the CO signal (black line), which is the most representative for the CO oxidation process, with the diffraction signal from both the Pt(111) surface (grey line) and α-PtO_2 layer (black line) shows that at the pulses "a" to "c" we measure high reactivity and a full oxide layer on the surface. At the pulses "d" and "e" we see a strong oscillation in the Pt(111) diffraction intensity, and a temporary decrease of the diffracted intensity from the oxide layer. This indicates that during the initial part of the pulse only a 'sub-monolayer' part of the initial oxide layer is left on the Pt(111) surface. At "f" the CO pulse is large enough to fully reduce the oxide layer: the oxide signal goes to 0 and the signal from the Pt(111) surface increases strongly. Simultaneously the reactivity decreases strongly. At "g" the reactivity regains its values expected for an oxidized surface, and the diffracted intensity from the Pt(111) surface shows a sharp step down. Only 10 – 20 minutes later we see a reappearance of the diffracted intensity from the oxide layer.*

3.5: Reaction rate and reactivity of α-PtO_2

We define the reaction rate *R(t)* as the amount of reaction product produced per unit time by the catalyst surface. As this is a closed "batch" reactor, and all produced gas remains inside the reactor, we can determine *R(t)* from the change in CO_2 pressure as a function of time. Fully equivalent to this, we can also determine *R(t)* from the decrease in CO pressure as a function of time, or the decrease in O_2 pressure[iii]:

$$R(t) = {d(P_{CO_2})}/{dt} = -{d(P_{CO})}/{dt} = 2 \cdot \left(-{d(P_{O_2})}/{dt} \right) \qquad (3a)$$

The change in P_{CO} during the pulses "a" to "e" in figure 11 clearly follows an exponential decay as a function of time. Putting a generic exponential decay function for P_{CO} into equation (3a) yields for *R(t)*:

$$R(t) = -{d(P_{CO})}/{dt} = {-d\left(A \cdot e^{-t/\tau} \right)}/{dt} = {A}/{\tau} \cdot e^{-t/\tau} \qquad (3b)$$

$$R(t) = {1}/{\tau} \cdot P_{CO}(t) = c \cdot P_{CO}(t) \Leftrightarrow R(P_{CO}) = c \cdot P_{CO} \qquad (3c)$$

Equation (3c) shows that during the pulses "a" to "e" the reactivity scales linearly with P_{CO}. The dependence of the reaction rate on P_{O2} is more difficult to determine. The oxygen pressure also decreases during these pulses as a function of time and as this is a batch reactor, the oxygen pressure follows the same exponential decay as the CO pressure. But the total oxygen pressure before and at the end of each pulse is much greater than the pulse itself. This means that the relative variation in the total oxygen pressure is relatively small (< 5%). Because of this, it is very difficult to determine the dependence of the reaction rate on the oxygen pressure during one single pulse. But by comparing the

[iii] *As the CO oxidation runs according to $2CO + O_2 \rightarrow 2CO_2$, two CO_2 molecules are produced from one single O_2 molecule. This means that the production rate of CO_2 is twice that of the decrease rate of O_2, hence the factor 2 in equation (2a).*

reaction rate from one pulse to the next during the pulses "a" to "e" we *can* determine the reaction rate as a function of P_{O2}. In figure 12a we have superimposed several different $P_{CO}(t)$ curves from the pulses "a" to "e". This shows that for different oxygen pressures during the different pulses, we find exactly the same reaction rate for the same value of P_{CO}. We conclude from this, that in these conditions, and for this variation in oxygen pressure the reaction rate is fully independent of P_{O2}.

As during the pulses "a" to "c" the surface is at all times fully covered by the Pt-oxide layer, the reaction rate found there is a good measure for the reactivity of the oxide surface. The reactivity is defined as the number of CO_2 molecules produced per site, per second on this surface at this temperature. As the exact reaction sites are unknown on this surface, we assume that each unit cell of the α-PtO_2 can provide one oxygen atom for a CO molecule to bind to. We can then calculate this number by dividing the reaction rate $R(t)$ in molecules per second

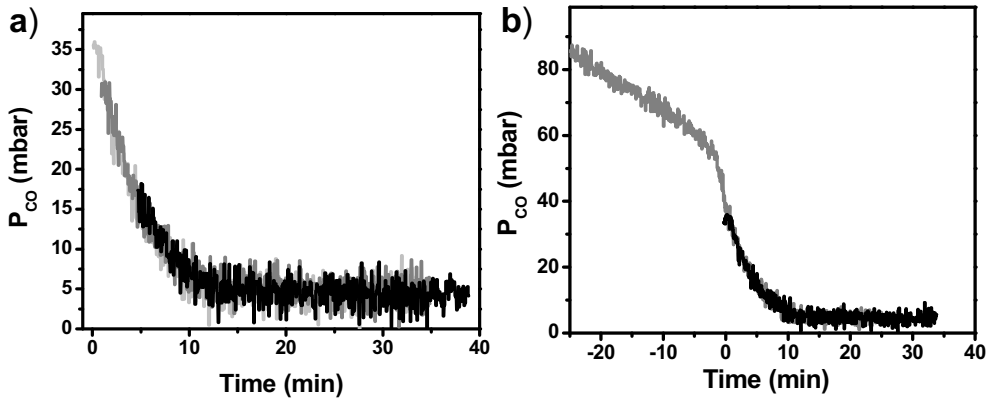

Figure 12: a) *CO pressure as a function of time for pulses "a" (black), "c" (grey) and "d" (light grey) of figure 10 superimposed (T = 600 K). The oxygen pressure differs almost 20% between the pulses a and d. As the catalyst exhibits the exact same reaction rate for the same CO pressure at all pulses, we conclude that the reaction rate is independent of the O_2 pressure in the high reactivity case (i.e. when the surface is oxidized).* ***b)*** *The CO pressure at point "g" from Figure 10 superimposed with the CO pressure from pulse "d" from that same experiment. Again we see the exact same reaction rate for the same CO pressure. The fact that we measure exactly the same reaction rate on the oxide and on the commensurate (2x2) layer confirms the conclusion that the reaction rate is not limited by the intrinsic reactivity of the surface, but only by the CO pressure, and i.e. the diffusion of CO towards the catalyst surface through the O_2-dominated gas phase.*

by the total available surface and multiply by the unit cell size of α-PtO_2. The highest value for the reactivity measured during the pulses "a" to "c" was $5.9 \cdot 10^2$ molecules/site/second at 20 mbar of CO and 610 K[iv].

3.5.1: Pulses "d" and "e"

When exposing the surface to pulses of CO in the order of 20 to 40 mbar (figure 11 "d" and "e") we see much stronger variations in the diffracted intensity coming from the Pt(111) substrate (figure 11b grey line). These variations have the typical shape already seen during the initial growth of the oxide layer, when Pt atoms were removed from the (111) surface causing so-called growth oscillations. These intensity oscillations are believed to again originate from Pt atoms being added or removed from the outermost Pt(111) layer. As the oxide surface is exposed to larger and larger pressures of CO, the reactivity becomes higher, as it scales linearly with the CO pressure. On the other hand the rate at which the reduced Pt atoms of the oxide layer are being re-oxidized remains unchanged, as the oxygen pressure only varies moderately. If during the peak of the CO pulse the reactivity is higher than the oxidation rate, suddenly a large part of the oxide layer can be reduced. If during such an event almost all the oxide is reduced, and only a fraction of a monolayer remains, we find the surface in the situation described in figure 6. The diffracted intensity from the oxide layer will be strongly reduced (figure 11b "d" and "e", black line). This partial coverage of less than one full monolayer by the oxide will also cause a strong variation in the diffracted intensity from the Pt(111) surface (figure 11b "d" and "e", grey line). After a fair part of the CO is consumed and the reactivity drops below the oxidation rate, the oxide layer grows back to its original value, as does its diffracted intensity. The diffraction intensity from the Pt(111) substrate does not recover completely. This can be due to the exact percentage of (metallic) Pt atoms in the interface layer between the oxide and the Pt bulk, or to roughness and disorder induced by the reduction and subsequent re-oxidation of the oxide layer. Both have the same effect on the diffracted intensity coming from the Pt(111) substrate and

[iv] *There is a small difference between the temperature stated here and the one stated for the whole pulse experiment. Because of the strong exothermity of the CO oxidation reaction, the sample heats up due to the reaction. The temperature during a pulse, and hence during a moment of high reaction rate, rises several degrees K. After all CO from one single pulse has reacted to CO_2 the temperature returns to the set value of 540K.*

we cannot differentiate between both solely on the data gathered in this experiment.

The peak reactivity measured during these two pulses is of $1.0 \cdot 10^3$ molecules/site/second at 33 mbar CO. This reactivity is exactly equal to the one found for the pulses a to c, given the relation $R(P_{CO})$ found in equation 3c. This is surprising as the variation in diffraction intensities shown in figure 11b suggests that only a fraction of a the surface was covered with α-PtO_2 during this pulse. We hence get the same reaction rate for only a fraction of the surface oxidized, and thus for a lower number of sites available for the reaction. This shows that the actual reactivity for a fully oxidized surface must be higher than the values calculated here above. A direct consequence of this observation is that the maximum value found for the reactivity, and hence the maximum reaction rate is not limited by the intrinsic reactivity of the catalyst surface. If the rate limiting step is not a process on the surface of the catalyst, it must be a factor from the gas phase which limits the reaction rate. The gas phase is dominated by oxygen, and the impingement rate of O_2 molecules onto the surface at this pressure and temperature is in the order of 10^9 molecules/site/second. Since this number is much higher than the reaction rate, this can not be the rate limiting factor. The impingement rate of CO, the minority species in the gas phase, must hence be the rate limiting step. This cannot be explained by the measured partial pressure of CO, as also that would lead to an impingement rate orders of magnitude higher than the measured reactivity. The only step that could limit the reaction rate is the diffusion of CO to the catalyst surface through the predominant O_2 environment. As a pulse of CO is introduced into the reactor, the very fast conversion of CO to CO_2 will deplete the surroundings of the catalyst surface of CO. From then on the reaction rate will be limited by the diffusion of CO from other parts of the reactor towards the catalyst surface. The oxide layer on the Pt(111) surface acts as an “unlimited” supply of atomic oxygen from the surface and is continuously replenished from the gas phase, which near the surface is composed for almost 100% O_2. This scenario is in perfect agreement with the linear dependence of the reaction rate on the CO pressure, and with the fact that it is fully independent of the oxygen pressure. This is also in full agreement with the fact that the reactivity is not affected by the exact coverage of the α-PtO_2 layer in the submonolayer range, as long as the coverage is non-zero. A calculation of the diffusion of CO through O_2 at these temperatures using Fick’s first law

confirms that the values found for the reactivity are indeed equal to the maximum impingement rate of CO in these conditions (see chapter 2.4.1).

The arguments stated here above conclusively show that the CO oxidation reaction on the oxidized Pt(111) surface is, in these conditions fully diffusion limited. We can state that the intrinsic reactivity of the oxidized Pt(111) surface under the presented reaction conditions must be significantly larger than 10^3 molecules/site/second.

3.5.2: Surface Structure and reactivity at pulse "f"

At pulse "f" in figure 11b the intensity from the α-PtO_2 layer drops to 0. Simultaneously we see a strong increase of the signal coming from the metal surface. This shows that the whole surface has been reduced, and is now back in a bulk terminated, metallic state, with a mixture of CO and atomic or molecular oxygen adsorbed to it. Simultaneously with this strong change in surface structure and composition we see a change in reaction rate. The reaction rate, calculated from equation 3c is a factor 10 lower than would have been expected for the oxide covered surface, i.e. for the diffusion limited case. Next to this strong decrease in reaction rate, we also observe that the reaction rate is no longer linearly dependent on the CO pressure. P_{CO} decreases almost linearly in time, indicating a much weaker dependence on the CO pressure. As *both* the reaction rate *and* the oxygen pressure are almost constant with time, it is very difficult to determine what the dependence of the reaction rate is with respect to P_{O2}. In figure 11a, with a zoom around points "f" and "g", we see a slight deviation in $P_{CO}(t)$ from true linear behavior. The reaction rate slightly *increases* as the CO pressure drops, and hence the CO/O_2 ratio drops. A metallic, gas covered surface on which the reaction rate depends on the CO/O_2 ratio would be consistent with a Langmuir-Hinshelwood (LH) reaction mechanism, as has often been proposed for CO oxidation on Pt catalysts [2,3,60]. In an ideal LH-type reaction the surface exhibits a maximum in reactivity when a 50% - 50% coverage for both reacting species is reached. In our experiment this corresponds to 50% CO and 50% atomic oxygen. Again in an ideal case, these coverages are directly linked to the partial gas pressures of both reactants. The fact that the reaction rate *increases* when the CO/O_2 ratio in the gas phase *diminishes* indicates that even with this relatively low CO/O_2

ratio, there is too much CO adsorbed on the surface. We hence conclude that the catalyst is in the so called "CO-poisoned" state [2,3,60].

At point "g" in figure 11 the CO/O_2 ratio drops below a certain threshold value, and the reaction rate suddenly increases. The reaction rate also reverts to the exponential decay, previously observed when the surface was oxidized. Together with the increase in reactivity we see a sharp step down in the diffracted intensity from the Pt(111) surface. This step is relatively modest with respect to the intensities measured when the surface is covered with α-PtO_2. The decrease in the diffracted intensity from the Pt(111) surface at point "g" is stepwise, and not gradual as is observed during oxide growth. Approximately 10 minutes after point "g", the diffraction signal from the α-PtO_2 oxide layer starts regaining intensity, indicating that the oxide layer starts reforming on the surface. This happens at a point when almost all CO has already been consumed. This means that the high catalytic activity before "f" can be attributed to the presence of the oxide layer in combination with the MvK mechanism. The low catalytic activity between "f" and "g" can be linked to the removal of the oxide layer and hence to the reaction running on the metallic surface. The high reactivity after "g", but *before* the reappearance of the oxide signal, can with this data not be linked to either the α-PtO_2 oxide layer, or the reduced, metallic surface.

3.6: 2x2 commensurate structure

In the time lapse between "g" and the regrowth of the α-PtO_2 oxide layer, the catalyst does exhibit a high reaction rate. However, according to the measurement shown in figure 11b, no other structural changes than a small decrease in the diffracted intensity from the Pt(111) surface are observed. When exploring a larger part of reciprocal space than just the exact (*h k l*) coordinates corresponding to the Pt(111) surface and the α-PtO_2 layer, we show that the surface does undergo a strong structural change, which exactly coincides with the sudden increase in reactivity observed at "g". Figure 13a (top panel) shows a series of in-plane scans along the ***K*** axis, plotted as a function of time, instead of as a function of ***K*** (see for comparison figure 2). Together with these scans, which show both the diffraction signal from the oxide and the Pt(111) surface, we have plotted the CO and CO_2 pressures (bottom panel).

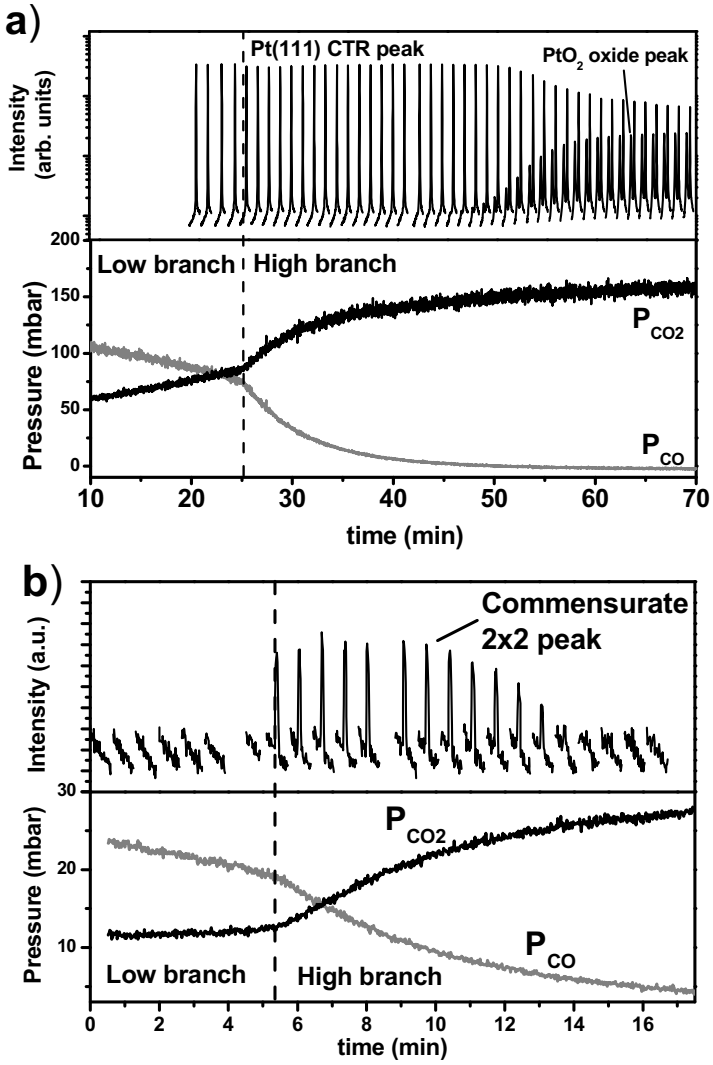

Figure 13: a)*: Repeated scans along the* ***K*** *direction around (1 -1 0.5) in 480 mbar O_2 at 570 K after a pulse of CO of 130 mbar. It captures both the diffraction from the Pt(111) CTR and from the α-PtO_2 layer. They are plotted as a function of time during the switch from the reduced, low reactivity state and the 'oxide', high reactivity state. A modest, but stepwise lowering of the Pt(111) peak is visible exactly at the moment the surface switches from low to high reactivity (dashed line). A more important but gradual decrease is visible approximately 25 minutes later, coinciding with the appearance of the diffraction signal from the α-PtO_2 layer.* ***b)****: CO and CO_2 pressures (resp. grey and black lines) as a function along the same time axis. The dashed line indicates the switch from low (left) to high (right) reactivity. b) top panel: Repeated scans along the* ***K*** *direction around (0.5 -0.5 0.5) in 500 mbar O_2 at 495 K after a pulse of CO of 150 mbar. It captures the diffraction signal from the 2x2 commensurate layer. The diffraction signal shows a stepwise increase to full intensity at the exact moment the surface switches from low to high reactivity, indicating that the whole surface is instantaneously covered with this structure. This allows us to directly link the elevated reactivity with the presence of this structure on the surface.*

We see a modest step down in intensity of the Pt surface signal exactly at the moment the reactivity switches from low to high (mind the log scale in comparison with the drop in intensity observed in figure 11b).

This indicates that simultaneously with the increase in reactivity, in a timeframe of less than one scan, a structural change occurs on the Pt surface. We also see the delayed regrowth of the oxide layer after approximately 20 minutes, as previously observed in figure 11b. The growth of the oxide can hence not be correlated with the change in surface structure which takes place exactly as the catalyst switches from high to low reactivity.

The experiment is repeated in figure 13b. We see the switch from the low reactivity (metallic surface) to the high reactivity. Again we combine the data from the online gas analysis with a series of scans along the **K** direction. A different part of reciprocal space has now been observed during the switch from low to high reactivity. The scan shown in figure 13b is a scan around a half-integer value of **K**. We see that a new diffraction peak appears immediately as the reactivity switches at exactly **K** = 0.5. In similar "switch" experiments not shown here peaks have been observed to appear at the positions **H** or $\mathbf{K} = n \cdot 0.5$ with $n = 1, 2, 3\ldots$. These peaks correspond to a commensurate structure, with a surface unit cell exactly twice as large as a Pt(111) unit cell,

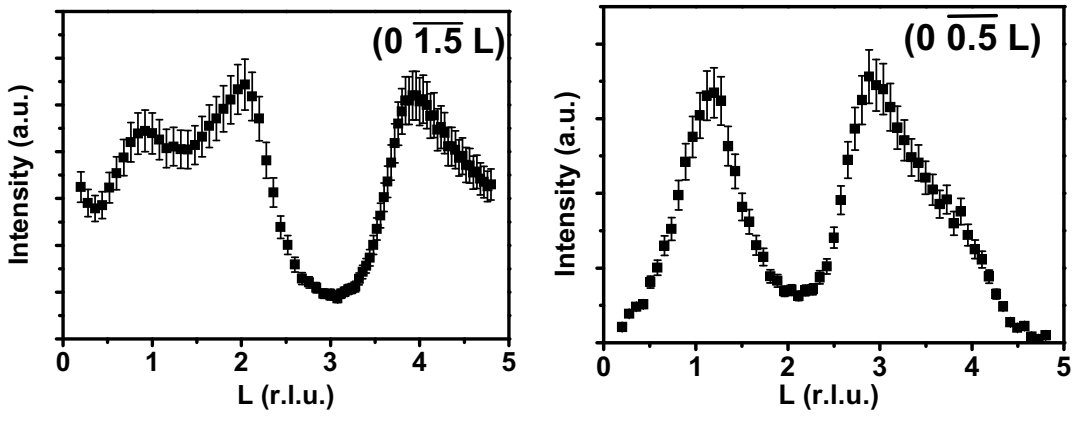

Figure 14: *Distribution of diffracted intensity along the **L** direction for two non-equivalent superstructure rods of the 2x2 layer. The strong oscillation in intensity as a function of **L** indicates that more than one layer of Pt is involved in this 2x2 structure. Despite the gathered dataset, the structure of this layer has not been elucidated.*

forming a (2x2) unit cell. To investigate this structure, a dataset of 5 non-equivalent in-plane reflections has been measured. The out-of-plane diffraction intensity has also been measured for 5 of these diffraction positions. For two of these positions, the out-of-plane intensity has been plotted as a function of **L** in figure 14.

Despite this relatively complete dataset, the exact structure and unit cell of this (2x2) commensurate layer has not been elucidated. The varying spacing of the out-of-plane diffraction maxima seen in figure 14 could not be reproduced with any know type of stacking (abc, abab, aaa etc). Educated guesses using linear combinations of these types of stacking have also failed to reproduce the measured reconstruction rods. The dataset was not extensive enough to be solved by direct method calculations [40].

From the coincidence of the appearance of this commensurate structure with the increase in reactivity, we conclude that this commensurate layer is responsible for the increase in reactivity. The reactivity for CO oxidation on the surface covered with this structure is, within the experimental error bars, the same as for the α-PtO_2 layer. This implies that again, the rate limiting factor is not the intrinsic reactivity of the layer itself, but the diffusion of CO through the O_2-dominated atmosphere to the surface. This also explains that again, similarly as with the α-PtO_2, the CO pressure drops exponentially in time, and reaction rate is hence again linear with the CO pressure.

3.7: Conclusions

We have shown that in an elevated pressure environment of mainly O_2 and elevated temperature conditions, an incommensurate α-PtO_2 layer form on the Pt(111) surface. The growth(rate) and thickness of this layer depend strongly on the O_2 pressure and temperature. At pressures in the order of 1 to 10 mbar of pure O_2, the growth of the layer is clearly accelerated by the presence of the X-Ray beam, probably due to the formation of ozone, a more oxidizing gas than pure oxygen. At pressures above 100 mbar, the growth is much faster, and no longer shows a clear beam effect.

Under these high pressure and temperature conditions this oxide layer exhibits a much higher reaction rate for catalytic CO oxidation than the (gas covered) metallic surface. This observation is in contradiction with the common knowledge assumption that oxide formation would “poison” a Pt catalyst for CO oxidation.

When going from a reducing to an oxidizing environment, hence form CO rich to a CO poor conditions, we see a stepwise, spontaneous increase of the reaction rate. This spontaneous increase can be linked to the formation of a commensurate (2x2) layer on the Pt(111) surface. This layer exhibits the same reactivity as the oxide layer. This reactivity is limited by CO diffusion towards the catalyst surface, and not by one of the catalytic conversion of CO to CO_2 on the catalyst surface. We conclude from this that the both the (2x2) and the oxide layer have a much higher reactivity than the metallic surface, but that we are insensitive to the intrinsic reactivity of the surface itself. We can only conclude that the intrinsic reactivity is higher than the values measured here above.